

Oligomeric organization of the B-cell antigen receptor on resting cells

Jianying Yang¹ & Michael Reth¹

B lymphocytes are activated by many different antigens to produce specific antibodies protecting higher organisms from infection. To detect its cognate antigen, each B cell contains up to 120,000 B-cell antigen receptor (BCR) complexes on its cell surface. How these abundant receptors stay silent on resting B cells and how they can be activated by a molecularly diverse set of ligands is poorly understood¹. Here we show, with the use of a quantitative bifluorescence complementation assay (BiFC)^{2,3}, that the BCR has an intrinsic ability to form oligomers on the surface of living cells. A BCR mutant that fails to form oligomers is more active and cannot be expressed stably on the B-cell surface, whereas BiFC-stabilized BCR oligomers are less active and more strongly expressed on the surface. We propose that oligomers are the autoinhibited form of the BCR and that it is the shift from closed BCR oligomers to clustered monomers that drives B-cell activation in a way that is independent of the structural input from the antigen.

The BCRs of all major immunoglobulin classes (IgM, IgD, IgG, IgE and IgA) form a complex comprising the transmembrane-bound immunoglobulin (mIg) molecule and the Ig α -Ig β heterodimer signalling subunits⁴. The cytoplasmic tails of Ig α and Ig β both contain an immunoreceptor tyrosine-based activation motif (ITAM) with tyrosine residues that are phosphorylated by the protein tyrosine kinases Lyn and Syk⁵. Because the BCR is not activated by soluble monovalent ligands, the current model of BCR activation entails crosslinking of at least two BCR complexes that results in the reciprocal phosphorylation and activation of ITAM-bound kinases leading to BCR activation. However, on closer examination, the crosslinking model has several problems. First, the monomeric BCR complex contains two ITAMs (that of Ig α and Ig β) and thus could place two associated kinase molecules in close proximity to each other without crosslinking. Second, the BCR is activated by structurally highly diverse ligands, which would not always be expected to place the two BCR monomers in the right conformation for reciprocal kinase phosphorylation. Third, this model does not attribute any role to the evolutionarily highly conserved amino acids in the transmembrane region of the mIg molecule apart from those involved in the binding of the Ig α -Ig β heterodimer. In a biochemical study, we previously detected oligomeric forms of the BCR and suggested that it is the opening of closed BCR oligomers by antigen rather than crosslinking that results in BCR activation^{1,6}. This model was challenged by a fluorescence resonance energy transfer (FRET) study with yellow fluorescent protein (YFP)-tagged and cyan fluorescent protein (CFP)-tagged BCR components, concluding from the low Ig α :Ig α FRET value that the BCR on living cells is a monomer^{7,8}.

To show that the BCR has an oligomeric organization on living cells, we first chose a synthetic biology approach, namely rebuilding the BCR in S2 *Drosophila* Schneider cells⁹ and monitoring the receptor with the BiFC method^{2,3}. A BCR is efficiently transported onto the

S2 cell surface only if all of its four components (membrane-bound heavy chain (mHC), lambda light chain (λ -LC), Ig α and Ig β proteins) are expressed together (Supplementary Fig. 1). Thus, the quality control of the endoplasmic reticulum seen in B cells is also active in S2 cells. In all our experiments we expressed BCR specific for the hapten 4-hydroxy-3-iodo-5-nitrophenylacetyl (NIP). The BiFC method monitors the dimerization of tagged proteins by means of the assembly of a complete YFP (cYFP) domain from the amino-terminal and carboxy-terminal half-domains of YFP (YN) and CFP (CC), respectively. To monitor the proper assembly and expression of the Ig α -Ig β heterodimer in living S2 cells, we co-expressed truncated forms of Ig α and Ig β carrying the YN and CC half-domains, respectively instead of a C-terminal tail. After 12 h of co-expression of the BCR components, we detected the cYFP fluorophore at the plasma membrane, indicating that the co-expressed Ig α -YN and Ig β -CC proteins formed a stable dimer that was transported as part of the BCR onto the S2 cell surface (Fig. 1a and Supplementary Fig. 2a). To test for the formation and localization of a BCR oligomer, we expressed the mIgM molecule in combination with wild-type (WT) Ig β and two forms of truncated Ig α carrying either the YN or the CC half-domain at the C terminus. In this experiment we also found an efficient accumulation of the cYFP chromophore at the plasma membrane, indicating a stable expression of an oligomeric BCR complex on the S2 cell surface (Fig. 1b and Supplementary Fig. 2b). As a negative control for these experiments, we co-expressed an IgM-BCR complex containing the Ig α -YN protein together with a chimaeric CD8 molecule carrying the CC half-domain as its cytosolic tail. S2 cells co-expressing these proteins formed only a small amount of the cYFP fluorophore. However, at the observed time point, the Ig α -YN-CD8-CC complexes formed did not accumulate at the S2 cell surface but were retained inside intracellular compartments (Fig. 1c and Supplementary Fig. 2c). This experiment was also conducted in B cells with the same results. Only Ig α -YN-Ig α -CC-containing BCR oligomers, but not Ig α -YN-CD8-CC-containing heterocomplexes, were stably expressed on the B-cell surface (Supplementary Fig. 3).

Once the fluorophore has formed, the YN and CC half-domains are covalently bound to each other. The assembly of the cYFP domain is thus an irreversible process. Given enough time, a cYFP domain could form even between low-affinity or non-specific binding partners². We therefore expressed the BCR for only 6 h under inducing conditions (0.1 mM CuSO₄) to avoid overexpression (Supplementary Fig. 4). To quantify the formation of cYFP within BCR complexes, we developed a new method based on the immunoprecipitation of multiprotein complexes detected by flow cytometry (IP-FCM)¹⁰. For this, we used latex beads coupled with the antigen NIP(15)-BSA to purify the NIP-specific BCR complexes from serial dilutions of digitonin lysates of the transfected S2 cells (Fig. 1d). Using phycoerythrin (PE)-labelled anti-Flag antibodies binding to

¹Centre for Biological Signalling Studies BIOS, Albert-Ludwigs-Universität Freiburg, Department of Molecular Immunology, Faculty of Biology, Albert-Ludwigs-Universität Freiburg and Max Planck Institute for Immunobiology, Stübeweg 51, 79108 Freiburg, Germany.

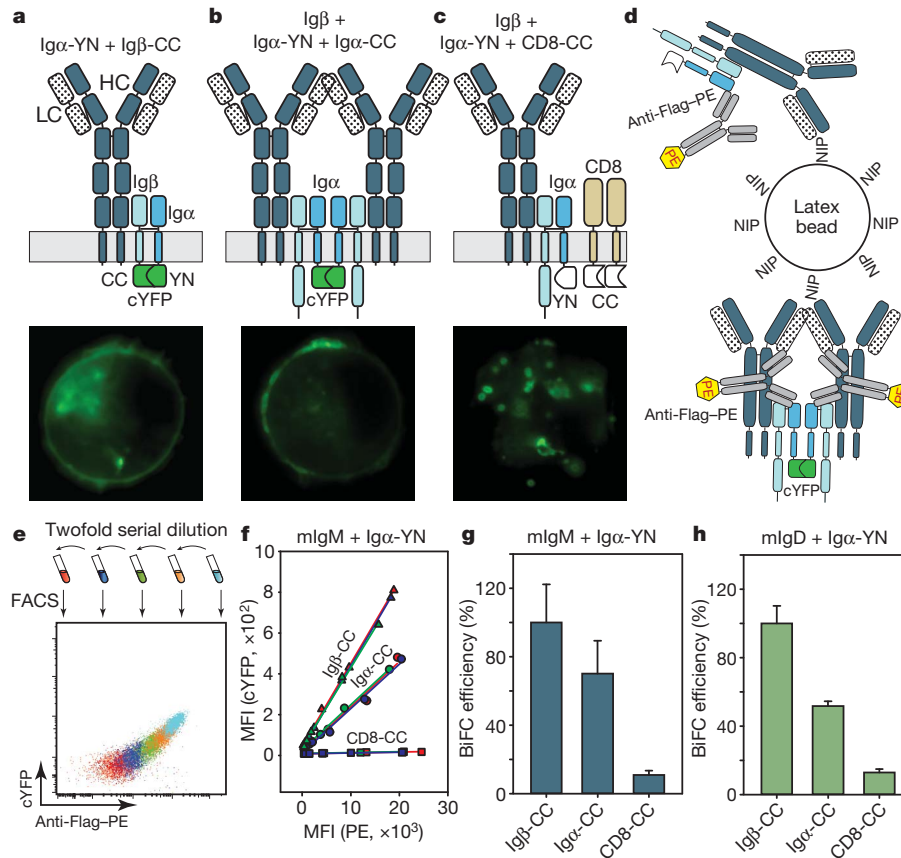


Figure 1 | BCR oligomers on S2 cell surface detected by BiFC and IP-FCM. **a–c**, S2 cells co-expressing the indicated receptor components for 12 h were harvested and analysed for the formation and localization of the cYFP domain by confocal microscopy. **a**, Localization of the Ig α /Ig β heterodimer in S2 cells co-expressing the mIgM molecule, the YN-tagged Ig α (Ig α -YN) and the CC-tagged Ig β (Ig β -CC). **b**, Localization of BCR oligomers in S2 cells co-expressing the mIgM and Ig β molecules as well as Ig α -YN and a CC-tagged Ig α (Ig α -CC). **c**, Localization of heterologous BCR–CD8 protein complexes in S2 cells co-expressing the mIgM and Ig β molecules together

with Ig α -YN and a CC-tagged CD8 molecule (CD8-CC). **d**, Schematic drawing of the application of IP-FCM. **e**, An overlay of the FACS analysis of the NIP(15)-BSA-coupled latex beads incubated with a series of five twofold dilutions of cell lysates after staining. **f**, An example of quantifying the BiFC efficiency by IP-FCM. For each sample, data from three independent experiments are shown (in red, green and blue, respectively). **g**, **h**, BiFC efficiency between the indicated partners in S2 cells expressing IgM–BCR (**g**) or IgD–BCR (**h**) complexes. Data are shown as means and s.e.m. for four independent experiments.

a Flag tag at the N terminus of Ig α , we used flow cytometry to measure the total amount of bound BCR and the protein–protein interaction within or between BCR complexes by means of the cYFP fluorophores formed (Fig. 1e). The mean fluorescence intensity of PE and YFP at different dilutions was then used to calculate the BiFC efficiency (Fig. 1f).

The formation of the Ig α -YN–Ig β -CC heterodimer in the IgM–BCR complex serves as a positive control in this analysis and we set its level of cYFP formation as 100% BiFC efficiency. High BiFC efficiency (about 50% to 70%) was also detected for the oligomerization of both the IgM–BCR and the IgD–BCR (Fig. 1g, h). The formation of the aberrant BCR–CD8 complex that is not expressed on the cell surface has a low (less than 15%) BiFC efficiency for both the IgM–BCR and the IgD–BCR. Note that in the Ig α -YN–Ig β -CC heterodimer, the (YN:CC) BiFC pairs are always placed next to each other, whereas BCR homodimers can also carry (CC:CC or YN:YN) pairs, which cannot make the complementation (Supplementary Fig. 2d). This explains the decreased (about 50%) BiFC efficiency of BCR oligomerization and may also be one of the reasons for the low FRET between BCRs containing Ig α -YFP and Ig α -CFP on the B-cell surface⁷.

To confirm that the formation of the Ig α -YN–Ig α -CC dimer measured by microscopy and IP-FCM reflects the interaction between fully assembled BCR complexes rather than the dimerization of unassembled Ig α , we co-expressed Ig α -YN and Ig α -CC with mIg in the absence of Ig β . In this case, the cYFP signal was retained inside the cell and no BiFC signal was detected by the IP-FCM method

(Supplementary Fig. 5). In addition, by conducting a multicolour BiFC assay¹¹, we showed that Ig α -YN–Ig α -CC complexes forming before the full assembly of the BCR were mostly retained inside the cells and were hardly detected by the IP-FCM assay (Supplementary Fig. 6). From this experiment we conclude that the observed high Ig α -YN–Ig α -CC BiFC efficiency indicates BCR oligomerization on the surface of living cells. A control supporting this conclusion was our finding that the cYFP fluorophore did not form in the cell lysates of the transfected S2 cells or on the latex beads (Supplementary Fig. 7).

Having developed a quantitative assay to monitor BCR oligomerization on living S2 cells, we employed this method to identify mutants that were defective in this process while still allowing the assembly of a BCR complex. The transmembrane part of mHC of different classes is highly conserved and is likely to form an α -helix with two functionally distinct sides¹. One side (TM-C) is conserved in all mHC classes and contains amino acids that bind to the transmembrane regions of the Ig α –Ig β heterodimer. The second side (TM-S) is class specific. Simultaneous mutation of six amino-acid residues on the δ m (membrane-bound δ HC) TM-S side including all hydrophilic residues (δ mTM-Smut) resulted in a reduction of the IgD–BCR oligomers to dimers as detected by a native gel analysis⁶. This finding suggests that the TM-S side of δ m is involved in BCR oligomerization. However, a comparison of IgD–BCR complexes containing either the WT or δ mTM-Smut in the S2 system did not show a difference in the BiFC efficiency of either Ig α –Ig β heterodimerization or BCR dimerization (Fig. 2a). This result is explained

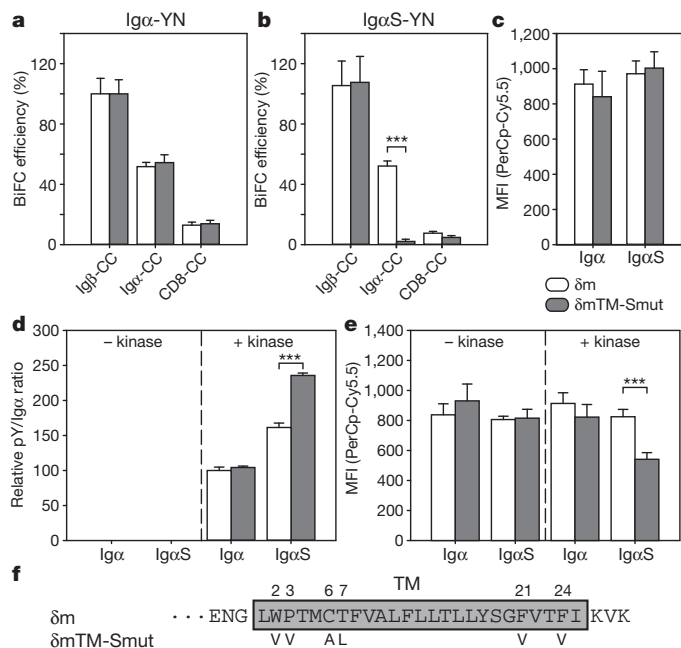


Figure 2 | **a** **double-mutant IgD-BCR complex without oligomerization.** **a, b**, BiFC efficiency between the indicated partners in S2 cells expressing the IgD-BCR complex containing either WT or mTM-Smut with YN-tagged WT (**a**) or mutant (**b**) Ig α . **c**, Comparison of the amount of BCR on the surface of S2 cells expressing WT, single-mutant or double-mutant IgD-BCR complex. **d**, Comparison of the phosphorylation of IgD-BCR expressed on the S2 cells, with or without the co-expression of Lyn and Syk kinases. The phosphorylation level was measured by IP-FCM and is represented as a phosphotyrosine (pY)/Ig α ratio. **e**, Comparison of the amount of BCR on the surface of S2 cells expressing IgD-BCR complexes with or without the co-expression of the kinases. Data are shown as means and s.e.m. for three independent experiments. Significant differences between samples: three asterisks, $P < 0.0001$. **f**, Sequence of δ m transmembrane region; the mutation sites are indicated.

by the fact that the TM-S mutated BCR still can form dimers; we therefore searched for additional mutations of BCR components that, in combination with the δ mTM-S mutation, would compromise dimer formation.

One of the mutations we tested was a cysteine-to-serine exchange in the linker region of Ig α (Ig α S), preventing the formation of a covalent disulphide bridge between the Ig α protein and the Ig β protein¹². This mutation, which probably makes the Ig α -Ig β heterodimer more flexible, did not change the BiFC efficiency of Ig α -Ig β heterodimerization or its incorporation into IgD-BCR complexes containing either WT or TM-Smut δ m chains (compare Fig. 2a with Fig. 2b). However, the BiFC efficiency of BCR oligomerization dropped drastically from 50% for the WT or single-mutant IgD-BCR to 5% for the double-mutant IgD-BCR complex (Fig. 2b). A fluorescence-activated cell sorting (FACS) analysis showed that 6 h after induction of receptor expression, WT, single-mutant or double-mutant IgD-BCR complexes were found in similar amounts on the S2 cell surface (Fig. 2c). Furthermore, in a kinetic study, we did not find any significant difference in the transport of WT or double-mutant IgD-BCR to the cell surface (Supplementary Fig. 8). This indicates that the double mutant can efficiently form an IgD-BCR complex although no BCR oligomers.

We next examined whether the defect of intrinsic oligomerization changes the signalling behaviour of the BCR. For this, we expressed WT or mutant IgD-BCR in S2 cells and monitored their tyrosine phosphorylation in the absence or presence of the protein tyrosine kinases Lyn and Syk by the quantitative IP-FCM assay. In the presence of the kinases, the double-mutant IgD-BCR showed increased tyrosine phosphorylation and decreased expression on the cell surface in comparison

with WT IgD-BCR (Fig. 2d, e). This shows that BCR complexes with defects in oligomerization are hyperactive and less stably expressed on the cell surface. BCR oligomers therefore seem to be an autoinhibited form of this receptor, the activation of which seem to be accompanied by conformational changes and an increased accessibility of the ITAM-containing tails. Such conformational changes have indeed been found for the T-cell antigen receptor (TCR)^{13,14}.

To test for the function of mutant IgD-BCR on the surface of B cells, we used the mIg-negative and Ig α -negative pre-B-cell line 3046 generated from the bone marrow of an Ig α and SLP65 double-knockout mouse¹⁵. The 3046 B cells were first transfected with retroviral vectors coding for the λ -LC and the δ m-HC (either WT or δ mTM-Smut). Those 3046 B cells producing an mIgD molecule were further transfected with a vector coding for either the Ig α WT or the Ig α S mutant. In the absence of Ig α protein, the mIgD molecules (WT and mutant) were not expressed on the 3046 B-cell surface (Fig. 3a, left panels). The restoration of a WT or single-mutant IgD-BCR complex on the 3046 B-cell surface (Fig. 3a, middle panels). However, the double-mutant (Ig α S + δ mTM-Smut) IgD-BCR complexes were expressed only at a lower level on the 3046 B-cell surface (Fig. 3a, lower right panel).

The decreased expression of double-mutant IgD-BCR on 3046 B cells could be due either to inefficient assembly or to increased internalization of this receptor. To study this in more detail, we developed an internalization assay employing a fluorescent peptide carrying only one NIP group (1NIP-peptide; Supplementary Fig. 9a). The 1NIP-peptide was efficiently bound by the NIP-specific BCR without stimulating it and this binding could be abolished by the free hapten NIP-CAP (Supplementary Fig. 9). To test for constitutive or induced internalization, we exposed B cells expressing either the single-mutant or double-mutant IgD-BCR to the 1NIP-peptide for 3 min in the absence or presence of anti-IgD antiserum. After this

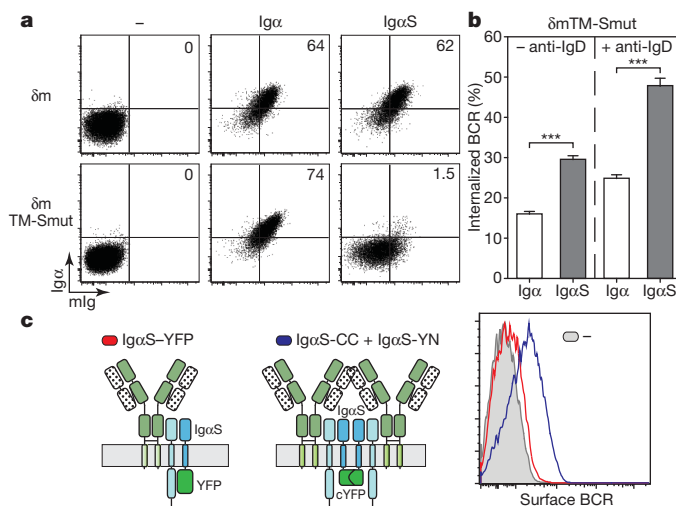


Figure 3 | **Monomeric BCR is not stably expressed on the B-cell surface.** **a**, FACS analysis of the expression of IgD-BCR complexes on the surface of 3046 B cells transfected with retroviral vectors that encode λ -LC and the indicated WT or mutant forms of δ m HC and Ig α . **b**, Comparison of the BCR internalization of 3046 B cells transfected with retroviral vectors that encode λ -LC, δ mTM-Smut HC and the indicated WT or mutant Ig α , with or without stimulation. The amount of internalized BCR is represented as a percentage of the amount of the surface BCR after 3 min of internalization. Data are shown as means and s.e.m. for four independent experiments. Significant differences between samples: three asterisks, $P < 0.0001$. **c**, FACS analysis of the expression of IgD-BCR complexes on the surface of 3046 B cells transfected with retroviral vectors that encode λ -LC, δ mTM-Smut HC and the indicated Ig α mutant fusion proteins. The grey area represents data from cells without Ig α . Data are representative of three independent experiments.

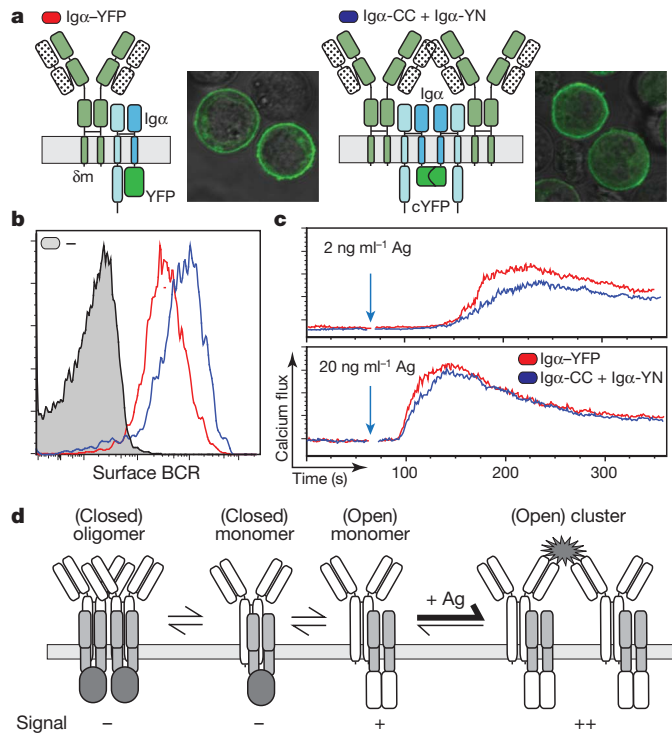


Figure 4 | Oligomeric BCR is highly expressed and autoinhibited. **a, b**, Schematic diagrams and representative confocal microscopy images (a) and FACS analysis (b) of the expression of IgD-BCR complexes on the surface of 3046 B cells transfected with retroviral vectors encoding λ -LC, δ m-HC and the indicated Ig α fusion proteins. The grey area represents data from cells without Ig α . Data in **b** are representative of three independent experiments. **c**, Calcium flux measured by FACS for cells expressing IgD-BCR containing Ig α -YFP or Ig α -CC-Ig α -YN after stimulation of the NIP(15)BSA antigen (Ag) at 2 or 20 ng ml $^{-1}$. Data are representative of three independent experiments. **d**, Schematic drawing of the dissociation activation model.

time we removed the 1NIP-peptide still bound to the surface with free hapten and measured the internalized peptide in a FACSscan. This study shows that, in comparison with the single mutant, the double-mutant BCR has an increased constitutive and anti-IgD-induced internalization rate (Fig. 3b).

The BiFC technique can be used not only to monitor receptor dimerization but also to stabilize receptor dimers. However, the latter method requires the constitutive expression of the reaction partners. Under these conditions we showed that the formation of an Ig α S-YN-Ig β -CC heterodimer (Supplementary Fig. 10) or an Ig α S-YN-Ig α S-CC homodimer (Fig. 3c) could, to a certain extent, restore the expression of a double-mutant IgD-BCR on the B-cell surface. In these experiments we used as control an Ig α -YFP fusion protein that also lacked the Ig α tail but could not participate in the BiFC reaction. Replacing the WT Ig α with this Ig α -YFP did not change the surface expression of the IgD-BCR (Supplementary Fig. 11). A direct comparison of unmutated IgD-BCR complexes containing either Ig α -YFP or the BiFC-stabilized Ig α -YN-Ig α -CC homodimer showed that the latter expressed larger amounts of IgD-BCR on the cell surface (Fig. 4a, b). However, in spite of its increased expression on the B-cell surface, the BiFC-stabilized IgD-BCR showed a decreased calcium response at low doses of antigen (Fig. 4c) and was also less well internalized than the Ig α -YFP containing IgD-BCR (Supplementary Fig. 12). This shows that BiFC-stabilized IgD-BCR oligomers behave completely differently from antigen-induced BCR clusters. It is therefore feasible that the former mimic the proposed autoinhibited BCR oligomers (Fig. 4d).

Currently, the BCR is studied mostly in its active state, whereas little is known about the conformation of the BCR before its exposure to

antigen. Using a new quantitative BiFC method, we found that in the absence of antigen, the IgM-BCR and IgD-BCR have an intrinsic ability to form oligomers on the surface of living S2 or B cells. A double-mutant IgD-BCR defective in BCR oligomerization but not in BCR assembly and transport was more readily phosphorylated and had an increased internalization rate. Our finding that a monomeric BCR was not stably expressed on the B-cell surface and was more active than an oligomeric BCR calls into question one of the major assumptions of the crosslinking hypothesis, namely that resting B cells express large amounts of signalling-inert monomeric BCR on their surface. Oligomeric forms have been found for the TCR¹⁶, and a recent study suggests that on resting T cells the TCR is preclustered and confined in lipid islands¹⁷. Similar structures have also been found on B cells¹⁸ and it is feasible that BCR oligomerization is required for its retention in such lipid islands. Furthermore, it has been shown that on resting B cells the BCR is associated with the cytoskeleton¹⁹.

The oligomeric organization of the BCR on the membrane of living cells suggests that it is more the dissociation than the aggregation of the BCR that drives B-cell activation. We propose a new dissociation activation model for BCR activation (Fig. 4d). According to this model, most of the BCRs on resting B cells form closed autoinhibited oligomers and the few BCR monomers that exist in an open, active conformation may provide a tonic survival signal^{20,21}. In the presence of antigen, the oligomer/monomer equilibrium of the BCR is shifted towards the more active monomer for signalling. Only a polyvalent antigen can keep the bound BCR monomers apart so that they can no longer form a closed oligomer. Because this (keeping-apart) function does not require a precise spacing of antigenic epitopes, it explains why so many structurally different soluble or membrane-bound antigens can activate the BCR^{22,23}. We think that the dissociation activation model explains the existing experimental data better than the crosslinking model. We hope that this improved model will suggest experiments that will finally result in a more profound understanding of BCR activation and a better treatment of immune diseases, particularly those that are caused by a hypoactive or hyperactive BCR²⁴⁻³⁰.

METHODS SUMMARY

Drosophila S2 cells (Invitrogen) and 3046 (Ig α $^{-/-}$ Slp65 $^{-/-}$) pre-B cells were propagated and transfected (see complementary vectors described in Methods) as described previously^{9,12,15}.

Transfected S2 cells were fixed 12 h after induced protein expression and mounted on slides (Marienfeld) before being imaged with a Zeiss 510 Meta confocal microscope (Carl Zeiss).

For quantitative IP-FCM, S2 cells were lysed with digitonin lysis buffer after 6 h of induced expression⁶. Five twofold serial dilutions of each cell lysates were immunoprecipitated by NIP(15)-BSA-coupled latex beads. After being washed with PBS, the beads were stained with antibodies and subjected to FACSscan. Samples with single staining were used to calculate the crosstalk between the fluorophores, and the data were corrected for the crosstalk before further analysis.

Cell-surface expression of the reconstructed BCRs was measured by FACSscan on an LSR II system (Becton Dickinson) after being stained. Calcium measurements were performed as described. Calcium flux was also measured with the LSR II.

Surface BCR internalization was determined by culturing the cells with 1NIP-peptide (IRIS Biotech) for 3 min. Surface-BCR-bound 1NIP-peptide was removed from the surface by incubating the cells with excess free hapten, and the internalized peptides were then measured by FACSscan on LSR II.

Full Methods and any associated references are available in the online version of the paper at www.nature.com/nature.

Received 11 February; accepted 14 July 2010.

Published online 5 September 2010.

- Reth, M. Oligomeric antigen receptors: a new view on signaling for the selection of lymphocytes. *Trends Immunol.* **22**, 356-360 (2001).
- Kerppola, T. K. Bimolecular fluorescence complementation (BiFC) analysis as a probe of protein interactions in living cells. *Annu. Rev. Biophys.* **37**, 465-487 (2008).
- Hu, C.-D., Chinenov, Y. & Kerppola, T. K. Visualization of interactions among bZIP and Rel family proteins in living cells using bimolecular fluorescence complementation. *Mol. Cell* **9**, 789-798 (2002).

4. Venkiteshram, A. R., Williams, G. T., Dariavach, P. & Neuberger, M. S. The B-cell antigen receptor of the five immunoglobulin classes. *Nature* **352**, 777–781 (1991).
5. Engels, N., Engelke, M. & Wienands, J. Conformational plasticity and navigation of signaling proteins in antigen-activated B lymphocytes. *Adv. Immunol.* **97**, 251–281 (2008).
6. Schamel, W. W. & Reth, M. Monomeric and oligomeric complexes of the B cell antigen receptor. *Immunity* **13**, 5–14 (2000).
7. Tolar, P., Sohn, H. W. & Pierce, S. K. The initiation of antigen-induced B cell antigen receptor signaling viewed in living cells by fluorescence resonance energy transfer. *Nature Immunol.* **6**, 1168–1176 (2005).
8. Tolar, P., Sohn, H. W. & Pierce, S. K. Viewing the antigen-induced initiation of B-cell activation in living cells. *Immunity. Rev.* **221**, 64–76 (2008).
9. Rolli, V. *et al.* Amplification of B cell antigen receptor signaling by a Syk/ITAM positive feedback loop. *Mol. Cell* **10**, 1057–1069 (2002).
10. Schrum, A. G. *et al.* High-sensitivity detection and quantitative analysis of native protein–protein interactions and multiprotein complexes by flow cytometry. *Sci. STKE* **2007**, pl2 (2007).
11. Hu, C.-D. & Kerppola, T. K. Simultaneous visualization of multiple protein interactions in living cells using multicolor fluorescence complementation analysis. *Nature Biotechnol.* **21**, 539–545 (2003).
12. Siegers, G. M. *et al.* Identification of disulfide bonds in the Ig- α /Ig- β component of the B cell antigen receptor using the *Drosophila* S2 cell reconstitution system. *Int. Immunol.* **18**, 1385–1396 (2006).
13. Minguet, S., Swamy, M., Alarcon, B., Luescher, I. F. & Schamel, W. W. Full activation of the T cell receptor requires both clustering and conformational changes at CD3. *Immunity* **26**, 43–54 (2007).
14. Gil, D., Schamel, W. W. A., Montoya, M., Sánchez-Madrid, F. & Alarcón, B. Recruitment of Nck by CD3 epsilon reveals a ligand-induced conformational change essential for T cell receptor signaling and synapse formation. *Cell* **109**, 901–912 (2002).
15. Meixlsperger, S. *et al.* Conventional light chains inhibit the autonomous signaling capacity of the B cell receptor. *Immunity* **26**, 323–333 (2007).
16. Schamel, W. W. *et al.* Coexistence of multivalent and monovalent TCRs explains high sensitivity and wide range of response. *J. Exp. Med.* **202**, 493–503 (2005).
17. Lillemeier, B. F. *et al.* TCR and Lat are expressed on separate protein islands on T cell membranes and concatenate during activation. *Nature Immunol.* **11**, 90–96 (2010).
18. Kim, J.-H., Cramer, L., Mueller, H., Wilson, B. & Vilen, B. J. Independent trafficking of Ig- α /Ig- β and μ -heavy chain is facilitated by dissociation of the B cell antigen receptor complex. *J. Immunol.* **175**, 147–154 (2005).
19. Treanor, B. *et al.* The membrane skeleton controls diffusion dynamics and signaling through the B cell receptor. *Immunity* **32**, 187–199 (2010).
20. Monroe, J. G. ITAM-mediated tonic signalling through pre-BCR and BCR complexes. *Nature Rev. Immunol.* **6**, 283–294 (2006).
21. Kraus, M., Alimzhanov, M. B., Rajewsky, N. & Rajewsky, K. Survival of resting mature B lymphocytes depends on BCR signaling via the Ig α / β heterodimer. *Cell* **117**, 787–800 (2004).
22. Kim, Y.-M. *et al.* Monovalent ligation of the B cell receptor induces receptor activation but fails to promote antigen presentation. *Proc. Natl Acad. Sci. USA* **103**, 3327–3332 (2006).
23. Harwood, N. E. & Batista, F. D. New insights into the early molecular events underlying B cell activation. *Immunity* **28**, 609–619 (2008).
24. Semichon, M., Merle-Béral, H., Lang, V. & Bismuth, G. Normal Syk protein level but abnormal tyrosine phosphorylation in B-CLL cells. *Leukemia* **11**, 1921–1928 (1997).
25. Pugh-Bernard, A. E. & Cambier, J. C. B cell receptor signaling in human systemic lupus erythematosus. *Curr. Opin. Rheumatol.* **18**, 451–455 (2006).
26. Peng, S. L. Altered T and B lymphocyte signaling pathways in lupus. *Autoimmun. Rev.* **8**, 179–183 (2009).
27. Payelle-Brogard, B., Magnac, C., Alcover, A., Roux, P. & Dighiero, G. Defective assembly of the B-cell receptor chains accounts for its low expression in B-chronic lymphocytic leukaemia. *Br. J. Haematol.* **118**, 976–985 (2002).
28. Lankester, A. C., Schijndel, G. M., Pakker, N. G., Van Oers, R. H. & van Lier, R. A. Antigen receptor function in chronic lymphocytic leukemia B cells. *Leuk. Lymphoma* **24**, 27–33 (1996).
29. Kawauchi, K., Ogasawara, T. & Yasuyama, M. Activation of extracellular signal-regulated kinase through B-cell antigen receptor in B-cell chronic lymphocytic leukemia. *Int. J. Hematol.* **75**, 508–513 (2002).
30. Chiorazzi, N. & Ferrarini, M. B cell chronic lymphocytic leukemia: lessons learned from studies of the B cell antigen receptor. *Annu. Rev. Immunol.* **21**, 841–894 (2003).

Supplementary Information is linked to the online version of the paper at www.nature.com/nature.

Acknowledgements We thank L. Leclercq, P. Nielsen, H. Jumaa and W. Schamel for critical reading of this manuscript. This study was supported by the Excellence Initiative of the German Federal and State Governments (EXC 294), by the Deutsche Forschungsgemeinschaft through SFB746 and by the FRISYS programme.

Author Contributions All experiments were planned by M.R. and J.Y. and conducted by J.Y. The manuscript was prepared by M.R. with J.Y.

Author Information Reprints and permissions information is available at www.nature.com/reprints. The authors declare no competing financial interests. Readers are welcome to comment on the online version of this article at www.nature.com/nature. Correspondence and requests for materials should be addressed to M.R. (michael.reth@bioss.uni-freiburg.de).

METHODS

Plasmids and retroviral vectors. The vectors for the expression of the BCR components in *Drosophila* S2 cells were described previously⁹. To construct the expression vector for the BiFC assay, DNA fragments coding for the N-terminal half (residues 1–172, YN) and the C-terminal half (residues 155–238, CC) of venus (Clontech) and eYFP (Clontech), respectively, were first amplified by PCR and cloned into the *Bam*HI/*Sal*I site of the S2 cell vector pRmHa-3 (ref. 9). A synthesized DNA fragment encoding the short linker sequence RSIATRS was then inserted into the *Bam*HI site upstream of the YN or CC coding sequence. Finally, the sequence encoding a Flag-tagged Ig α (residues 1–169), or haemagglutinin-tagged Ig β (residues 1–191) or CD8 α (residues 1–219) was amplified by PCR and inserted upstream of the linker.

To perform the BiFC assay in B cells, we used the 3046 pre-B-cell line with retroviral expression vectors as described previously³¹. Sequences encoding the BiFC plasmids were amplified by PCR and cloned into the respective retroviral vectors carrying different selection markers after the internal ribosome entry site (IRES). For the YFP-tagged Ig α , DNA fragments coding for venus (Clontech) were first amplified by PCR and cloned into the *Bam*HI/*Sal*I site of the S2 cell vector pRmHa-3. A synthesized DNA fragment encoding the short linker sequence RSIATRS was then inserted into the *Bam*HI site upstream of the venus coding sequence. Then, the sequence encoding a Flag-tagged Ig α (residues 1–169) was amplified by PCR and inserted upstream of the linker. Finally, the resulting sequence encoding Ig α -YFP fusion protein was amplified by PCR and cloned into the respective retroviral vectors.

For the reconstitution of the BCRs in 3046 pre-B cells, we used retroviral expression vectors as described previously³¹. Sequences encoding δ mTM-Smut and Ig- α S were amplified by PCR and cloned into the respective retroviral vectors.

Cell culture and transfection. For transient transfection, 3×10^5 *Drosophila* S2 cells from an exponentially growing culture were cultured for 24 h in 24-well plates. The different plasmids were mixed (0.1 μ g of each plasmid with the exception of the plasmid encoding the heavy chain, of where we used 0.15 μ g) and diluted in 40 μ l of serum-free medium. The amount of DNA was equalized with the empty vector pRmHa-3. After the addition of 40 μ l of serum-free medium containing 3 μ l of CellFectin (Invitrogen), the vector DNA was incubated for 10–15 min at 25 °C. The mixture was then adjusted to 250 μ l with serum-free medium and added to cells previously washed with serum-free medium. After incubation for 18 h, the solution was replaced with 1 ml of medium and the cells were cultured for a further 24 h. Plasmid encoding GFP was co-transfected when determination of the transfection efficiency was needed. For induction of gene expression, CuSO₄ was added to the culture at a final concentration of 1 mM for 12 h (for microscopic analysis) or 0.1 mM for 6 h (for quantitative BiFC with IP-FCM and FACScan analysis of cell surface expression) before collection of the cells.

The 3046 (Ig- α ^{-/-} Slp65^{-/-}) pre-B cells were maintained and transfected as described previously³¹.

Quantitative IP-FCM. Carboxylate Modified Latex (CML) beads with a diameter of 6 μ m (Interfacial dynamics) were coupled with NIP(15)-BSA (Biosearch Technologies) in accordance with the manufacturer's instructions. For measuring the BiFC efficiency, 10⁶ S2 cells were washed once with PBS and lysed in 150 μ l of 1% (v/v) digitonin lysis buffer⁶. Cell lysates were diluted with PBS in a U-form 96-well plate (Greiner Bio-one) and five twofold serial dilutions were made for each sample (Fig. 1e). To each dilution, 5×10^3 NIP(15)-BSA-coupled CML beads were added and incubated for 1 h at 4 °C. After being washed with PBS, the beads were stained with anti-Flag-PE antibody (1:100 dilution; Martek) for 15 min on ice and washed once with PBS. The amount of bound antibody and cYFP was measured in the FACScan. For measuring the ITAM phosphorylation, transfected S2 cells were lysed with digitonin and the BCR in the lysate was purified on NIP(15)-BSA-coupled CML beads with the same method. The beads were then stained with fluorescein isothiocyanate (FITC)-conjugated anti-phosphotyrosine antibody (4G10-FITC; 1:100 dilution; Upstate) to determine the phosphorylation level and with anti-Flag-allophycocyanin (APC) antibody (1:100 dilution; PerkinElmer) to determine the amount of BCR.

To quantify the IP-FCM data, FACS experiments were performed with the LSR II system (Becton Dickinson) and data were exported in FCS-3 format and analysed with Flowjo (Tree Star) software. Samples with single staining were used to calculate the crosstalk between the fluorophores; data were corrected for crosstalk before further analysis. To measure the BiFC efficiency, for each sample the mean fluorescence intensities of cYFP were plotted against the mean fluorescence intensities of anti-Flag-PE from its five dilutions (Fig. 1f). Although standard controls for quantifying each fluorophore were not available for each sample, one can clearly see a linear relationship between the two fluorophores (Fig. 1e, f), which measures the amount of total bound BCR and complemented cYFP, respectively. In this way, the BiFC efficiency can be quantified by fitting the data with a linear regression by using Prism (Graphpad) software. The calculated slopes were then normalized to the slope of the positive control and plotted as a bar plot with Prism. Similarly, to quantify the ITAM phosphorylation of the BCR, for each of the five dilutions of the lysate we performed a linear regression of the mean fluorescence intensity of 4G10-FITC bound to the CML beads plotted against the mean fluorescence intensity of anti-Flag-APC. Again, all further analysis was done with Prism.

Surface BCR internalization assay. 1NIP peptide (H-K(Dylight649)-S-K(NIP)-GESAG) with more than 95% purity (verified by HPLC) was purchased from IRIS Biotech. 3046 cells expressing WT or a mutant form of IgD-BCR were cultured to a concentration of $(1-2) \times 10^6$ cells ml⁻¹ before the assay. The cells were first diluted with fresh medium to 10⁶ cells ml⁻¹ and transferred to U-form 96-well plates (Greiner Bio-one). Each well was filled with 200 μ l of mixture (2×10^5 cells). The cells were then cultured in 37 °C incubator for 30 min before the assay. The cells were kept at 37 °C for 3 min after the addition of 10 μ l of the 4 μ M 1NIP peptide with or without anti-IgD antiserum (1:5 dilution; eBioScience), and the cells were collected and kept on ice. After being washed twice with FACS buffer (0.05% azide, 3% FCS in 1 \times PBS), 30 μ l of NIP-CAP (100 μ M) was added to the cells for 15 min on ice to remove the 1NIP peptide attached to the surface BCR. As control, two wells of the cells without the 3-min treatment of the peptide were stained with 1NIP peptide (20 μ l, 0.2 μ M) after the wash of FACS buffer, and one was also treated with NIP-CAP after the staining to check the surface BCR expression and the effect of the NIP-CAP. All the cells were washed again twice with FACS buffer and the internalized 1NIP peptide was measured by FACS on the LSR II. FACS data were then analysed with Flowjo.

Calcium measurement and flow cytometry. Calcium measurements were performed as described³¹. Cells (5×10^6) were stimulated with 2 or 20 ng ml⁻¹ NIP(15)-BSA. Calcium flux was measured with the LSR II. For FACS analysis of BCR surface expression in S2 and 3046 cells, cells were stained with anti-Flag-APC (1:100 dilution; PerkinElmer) for the Flag-tagged Ig α , or NIP(15)-BSA-biotin (1:400 dilution) and streptavidin-PerCP-Cy5.5 (1:200 dilution; Becton Dickinson) for the NIP-specific mIg, and measured with the LSR II. In certain cases, 1NIP peptide (0.2 μ M) was used for the surface staining to determine the expression level of NIP-specific BCR. Data were exported in FCS-3 format and analysed with Flowjo software.

Data processing and statistic analysis. Means and s.e.m. from three or four independent experiments were used for plotting with Prism software. To determine differences between data sets, a one-tailed unpaired *t*-test was performed. *P* values for each test are given in the corresponding figure legends.

Imaging. S2 cells were collected and washed with PBS 12 h after the induced expression of the BCR components. Cell pellets were then fixed with 2% paraformaldehyde (Sigma) and mounted on slides (Marienfeld) with Fluoromount-G (SouthernBiotech). A Zeiss 510 Meta confocal microscope (Carl Zeiss) was used for fluorescence microscopy. A Zeiss (Plan-Apochromat) 63 \times water-immersion objective lens was used for image acquisition. To reveal the BiFC in 3046 cells, cells were collected and washed with PBS 12 h after retroviral transfection of the cells with the BiFC plasmids. Cells (10⁶) were then resuspended in 800 μ l of PBS buffer and loaded on a 35-mm M-dish (Ibidi). A Zeiss (Plan-Apochromat) 63 \times oil immersion objective lens was used for image acquisition.

31. Storch, B., Meixlsperger, S. & Jumaa, H. The Ig- α ITAM is required for efficient differentiation but not proliferation of pre-B cells. *Eur. J. Immunol.* **37**, 252–260 (2007).